ISSN 0023-1584, Kinetics and Catalysis, 2009, Vol. 50, No. 2, pp. 247–254. © Pleiades Publishing, Ltd., 2009.
Original Russian Text © A.L. Lapidus, M.N. Mikhailov, I.V. Mishin, A.A. Dergachev, V.Z. Mordkovich, 2009, published in Kinetika i Kataliz, 2009, Vol. 50, No. 2, pp. 262–269.

Framework Composition and Activity of Platinum-Containing High-Silica Zeolites in *n*-Hexane Isomerization[1]

A. L. Lapidus[a], M. N. Mikhailov[a,b], I. V. Mishin[a], A. A. Dergachev[a], and V. Z. Mordkovich[b]

[a] *Zelinskii Institute of Organic Chemistry, Russian Academy of Sciences, Moscow, 119991 Russia*

[b] *United Research and Development Center, Moscow, 119333 Russia*

e-mail: mik@ioc.ac.ru

Received April 16, 2008

Abstract—The conversion of *n*-hexane on Pt-containing dealuminated mordenites and ZSM-5 zeolites was studied. The framework composition and the concentrations of extraframework aluminum compounds in mordenites were determined by X-ray diffraction analysis. It was demonstrated that the aluminum content of the framework affected the activity in *n*-hexane isomerization. It was found that a Pt-mordenite catalyst containing a considerable amount of extraframework aluminum compounds exhibited maximum activity. A quantum-chemical study of the interaction of platinum with Brønsted and Lewis acid sites was performed. It was hypothesized that oxidized surface platinum nanoparticles were the active sites of Pt-containing high-silica zeolites. These nanoparticles were formed by the interaction of platinum clusters with proton sites or extraframework aluminum compounds. An alternative mechanism was proposed for the conversion of alkanes to exclude the direct participation of acid sites.

DOI: 10.1134/S0023158409020153

INTRODUCTION

High-silica zeolites containing platinum are characterized by high activity in *n*-hexane isomerization [1, 2]. Zeolites of the ZSM-5 type with various framework compositions are prepared by crystallization, whereas the framework composition of mordenite can be varied over wide ranges by dealumination [3]. The removal of framework aluminum results in the development of a mesopore structure and the formation of extraframework aluminum (EFAL) compounds. In this case, the strength and concentration of Brønsted acid sites (BASs) change and Lewis acid sites (LASs) are formed [4]. According to the current concept of bifunctional catalysis, the steps of dehydrogenation and hydrogenation occur at a metal particle, whereas isomerization and carbon–carbon bond cleavage occur at an acid site. This implies the occurrence of two types of sites, which are independent of each other [5–7]. In studies on alkane isomerization on bifunctional catalysts, activity changes have usually been related to the concentration of BASs. Advances in bifunctional catalysts in Russia are intimately associated with the scientific activity of Academician Khabib Minachevich Minachev, a prominent scientist whose 100th birthday was celebrated in December 2008. As a young researcher, he worked under the supervision of N.D. Zelinskii in the science of catalysis, and his life's work centered on service to this science. The pioneering works of Minachev resulted in the discovery of the hydrogenating activity of the sodium forms of zeolites, the development of metal–zeolite catalysts for toluene hydrodealkylation, the single-step synthesis of methyl isobutyl ketone from acetone and hydrogen, the production of isoprene from isobutylene and formaldehyde, and the steam conversion of hydrocarbons into synthesis gas. Minachev achieved much success in studying catalytic reactions; he was interested in understanding the nature of catalytic effects. As a recognized scientist in organic catalysis, he became leader in works concerning the use of photoelectron spectroscopy in catalysis. These works allowed him to determine the nature of interactions between reacting atoms at the electron level. Minachev supported works oriented to study active sites using EPR spectroscopy and adsorption microcalorimetry, as well as quantum-chemical studies in adsorption and catalysis. The use of quantum chemistry methods, in particular, the density functional theory (DFT), allowed one to simulate interactions on the surface of a heterogeneous catalyst. Recently, Mikhailov et al. [8] found that the introduction of platinum into ZSM-5 zeolite was accompanied by the interaction of the metal with an acid site and proton transfer from a Brønsted site to a metal particle; this is consistent with experimental data on acidity measurements [9]. As a result, the platinum particle was oxidized and stabilized in a zeolite channel and the acidity of the support was suppressed. It was hypothesized that metal particles stabilized in zeolite channels were active sites in the conversion of alkanes on these catalysts, whereas BASs did not participate directly in the reaction. In this case, the role of LASs in the formation of active sites remains poorly

[1] Dedicated to the 100th birthday of Academician Kh.M. Minachev.

Table 1. Preparation conditions and compositions of zeolite supports

Zeolite	Preparation conditions	C_{Al}, atom per unit cell	
		framework	extraframework
HZSM(15)	NaZSM(15), 1N NH_4NO_3, 5 h, 550°C	5.9	0.05
HZSM(38)	NaZSM(38), 1N NH_4NO_3, 5 h, 550°C	2.4	0.03
HM(6)	NaM(6), 1N NH_4NO_3, 5 h, 550°C	6.5	0.3
HM(6)-650	NH_4M(6), 650°C	2.6	4.2
DHM(9.5)	NH_4M(6), 650°C, 2N HCl, 5 h, 100°C	1.3	3.0
DHM(25.5)	NH_4M(6), 650°C, 4N HCl, 5 h, 100°C	0.9	0.7
DHM(37.5)	NH_4M(6), 650°C, 6N HCl, 5 h, 100°C	0.7	0.4

understood. Zeolites like mordenite and ZSM-5 are convenient test materials for the determination of the roles of BASs and LASs in the conversion of alkanes on bifunctional catalysts. A special feature of mordenite is that both framework aluminum and EFAL atoms are present in dealuminated samples, and the concentration ratio between these atoms depends on the degree of dealumination. At the same time, ZSM-5 zeolites with different Si/Al ratios mainly contain framework aluminum atoms. In this work, we studied the effects of the framework composition and the ratio between the numbers of framework aluminum and EFAL atoms on the activity of Pt-containing zeolites in *n*-hexane isomerization.

EXPERIMENTAL

Preparation of catalysts. Mordenites prepared by direct synthesis and dealumination and ZSM-5 zeolites were used in this study. Table 1 summarizes the zeolite compositions and preparation conditions. The hydrogen forms of the zeolites were prepared by the treatment of the parent Na forms with an aqueous solution of NH_4NO_3 at 90°C followed by heating at 450°C. The mordenites were dealuminated by the treatment of the ammonium form of the zeolite preheated at 650°C with a 2–6 N HCl solution. In this work, the samples prepared by direct synthesis and the dealuminated mordenites are referred to as HM and DHM, respectively, and the Si/Al ratios in the samples are given in parentheses. The total silicon and aluminum concentrations in dealumination products were determined by X-ray fluorescence spectroscopy. The aluminum content of the framework was found by the X-ray powder method. Platinum was introduced into mordenites by impregnating the zeolite powders with an aqueous solution of H_2PtCl_6 followed by drying at 120°C and heating in a flow of air at 400°C for 2 h. Before catalytic experiments, the catalysts were granulated, and the granules were crushed; a fraction of 1–2 mm was taken and treated in a flow of hydrogen at 350°C with increasing temperature at a rate of 3 K/min for 2 h.

X-ray diffraction. X-ray diffraction was used to determine the relative crystallinity and composition of the framework. Analysis was performed on a DRON-2 diffractometer at a goniometer rate of 0.5 deg/min using CuK_α radiation and cerium oxide as an internal standard, which was added in an amount of 10 wt % with respect to the zeolite sample weight. The relative crystallinity was calculated from the intensity ratio between reflections from the mordenite plane [150] at $2\theta = 23.5°$ and the cerium oxide plane [111] at $2\theta = 28.57°$ taking the ratio between these intensities in the X-ray diffraction pattern of a reference sample of Na mordenite to be 100%. To determine the framework composition, the dependence of mordenite lattice parameters on the aluminum content of the framework was used; this dependence was described by the equation [10]

$$C_{Al} = (b - 20.209)/0.000347,$$

where C_{Al} is the number of Al atoms in the mordenite unit cell and b is the unit cell parameter, Å. The unit cell parameters were calculated from the angles of reflection of 20 diffraction peaks of mordenite in the region of $2\theta = 6°–50°$.

Catalytic activity. The reaction of *n*-hexane isomerization was performed in a flow system with a fixed catalyst bed at 0.1 MPa, 175–325°C, and an H_2/n-C_6H_{14} molar ratio of 5; the rate of hydrocarbon supply (v) was varied over the range of 0.01–0.08 mol h^{-1} g_{Cat}^{-1}. The products of *n*-hexane conversion were analyzed by GLC (30-m capillary column with the SE-30 phase, flame-ionization detector, and N_2 as the carrier gas). The activity of the catalysts was evaluated from the conversion of *n*-hexane (K) and the total yield of C_6 isomers (Y_i). To calculate the initial rates of isomerization V (mol h^{-1} g_{Cat}^{-1}), the linear portions of kinetic curves plotted in the $Y_i = f(1/v)$ coordinates were used at 10–15% conversions.

Table 2. Isomerization of *n*-hexane on platinum–zeolite catalysts (0.3 wt % Pt)

Catalyst	*T*, °C	*K*, %	Yield of products, %		
			ΣC_1–C_4	ΣC_5	Σiso-C_6
Pt/HZSM(15)	250	74.5	9.2	4.2	61.1
Pt/HZSM(38)	250	47.5	0.3	0.2	47.0
Pt/HM(6)	225	16.8	0.1	–	16.7
Pt/DHM(9.5)	225	66.2	0.9	0.6	64.6
Pt/DHM(25.5)	225	51.1	0.5	0.2	50.3
Pt/DHM(37.5)	225	37.2	0.3	0.1	36.8

Computational procedures. The cluster approach was used to describe the structures of zeolites. The electronic structures of the clusters were calculated by the DFT method using the exchange B3 functional [11] and correlation LYP [12] and VWN5 [13] functionals. The SBKJC pseudopotential [14] and the corresponding basis set augmented by the polarization functions on all atoms were used to decrease the computational time. All of the calculations were performed with the use of the quantum-chemical PC GAMESS program package [15, 16]. Natural site populations were analyzed using the NBO program package [17].

Two ten-membered rings arranged at the point of intersection of straight and sinusoidal channels were used as the basis for a cluster that simulated a fragment of the ZSM-5 zeolite framework. We considered two cluster models: one of them included 14 Si atoms and 1 Al atom, and the other included only Si atoms. The dangling bonds (Si–O and Al–O) of a cluster were saturated with hydrogen atoms arranged at distances of 1.6 and 1.5 Å along Al–O and Si–O bonds, respectively. All of the terminal H atoms were fixed in the course of geometry optimization. The excess negative charge of the lattice of the hydrogen form of a zeolite was compensated by a proton, which formed a BAS. The stoichiometry of the resulting clusters was $AlSi_{14}O_{18}H_{25}$ and $Si_{15}O_{18}H_{24}$, respectively. The EFAL species was simulated by the $Al_2O_2(OH)_2$ cluster.

RESULTS AND DISCUSSION

Table 1 specifies the preparation conditions, total composition, and framework composition of high-silica zeolites and the concentrations of EFAL compounds. In ZSM-5 zeolites, the framework composition can be changed over a wide range by varying the Si/Al ratio in the reaction mixture during crystallization. The experimental data indicate that the total compositions and framework compositions of the hydrogen forms of two ZSM-5 samples with Si/Al = 15 and 38 coincided; thus, almost all aluminum atoms in these samples occurred in the framework. Correspondingly, only BASs will participate in the formation of active sites for isomerization in these zeolites. Table 2 summarizes the results of the study of *n*-hexane isomerization on Pt/HZSM(15) and Pt/HZSM(38) catalysts; these data indicate that the activity of the samples decreased by a factor of almost 2 as the aluminum content of the framework was halved. C_1–C_5 hydrocarbons, which resulted from cracking, almost completely disappeared from the products of hexane conversion on the sample with Si/Al = 38. Usually, the decrease in the activity of ZSM-5 zeolites in acid-type reactions was related to a decrease in the number of BASs [18]. This regularity has been extended to Pt-containing zeolites assuming the independent catalytic effects of metal and acid sites. However, the metal–acid site interactions are ignored in the concept that alkane isomerization takes place only at BASs.

Our calculations suggest that the introduction of platinum into the hydrogen form of the zeolite resulted in the strong specific interaction of metal particles with BASs, as a result of which the acidity of the support was suppressed. Figure 1a shows the optimized structure of a cluster that simulates a platinum particle in the HZSM-5 zeolite. Table 3 summarizes the main parameters that characterize the electronic structures of an isolated Pt_6 cluster and a cluster adsorbed on zeolite framework fragments. In the electronic ground state, the isolated Pt_6 cluster has the geometry of a distorted octahedron (Pt–Pt bond lengths are 2.63, 2.66, and 2.97 Å) and it is characterized by a spin multiplicity of 9 (the $5d^{9.41}6s^{0.55}$ electron configuration). The adsorption interaction of this nanoparticle with HZSM-5 zeolite is characterized by an adsorption energy of 45 kcal/mol, and it leads to BAS proton transfer to the metal surface. The transfer is an exothermic (ΔE = –36 kcal/mol) and activation-free process. Proton transfer from the BAS (the $1s^{0.46}$ electron configuration) to the platinum particle results in the appearance of a positive charge (0.53) on the Pt_6 cluster because of a decrease in electron density on 6*s* orbitals. Electron-density transfer from framework Si and Al atoms to the metal particle through oxygen atoms simultaneously occurs in the system. The interaction of the platinum particle with the zeolite BAS is associated with the for-

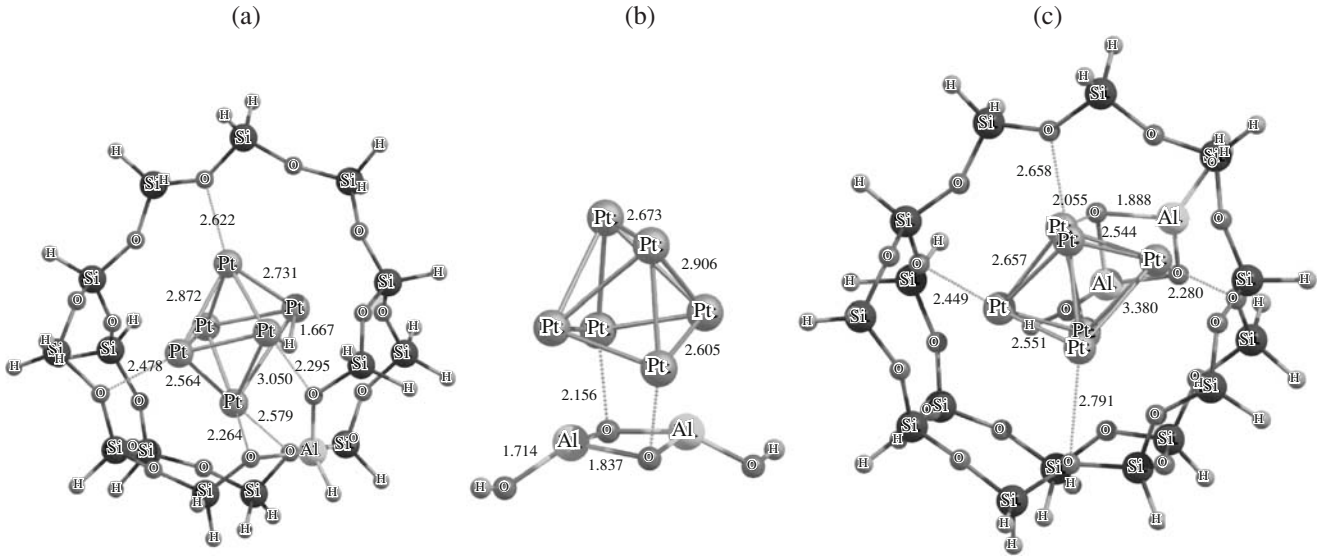

Fig. 1. Optimized structures that simulate the Pt_6 particle adsorbed (a) in a zeolite channel, (b) at the extraframework $Al_2O_2(OH)_2$ particle, and (c) at the extraframework $Al_2O_2(OH)_2$ particle in a zeolite channel.

mation of the complex cation Pt_6H^+, which occupies a cationic position. In this case, hydrogen occurs as an adsorbed hydrogen atom (the $1s^{0.99}$ electron configuration) rather than a proton on the surface of the positively charged metal particle. The Pt_6H^+ cluster is extended along the cross section of the zeolite channel. In the proton-transfer structure, the singlet and triplet states are almost degenerate: the singlet–triplet splitting is no higher than 3 kcal/mol. Table 3 indicates that, upon the introduction of the Pt_6 cluster into a channel of the hydrogen form of zeolite, the chemical potential (μ) of the metal particle decreases by more than 1 eV, whereas the hardness (η), which characterizes the change in the chemical potential under changes in the number of electrons [19], decreases by 0.33 eV.

Thus, the introduction of platinum into the hydrogen form of pentasil is accompanied by proton transfer from the BAS to the metal cluster surface. This results in the stabilization of the platinum particle in the zeolite channel, the oxidation of the metal particle (the formation of the $[Pt_6H]^+$ cation), and a considerable decrease in or even the complete suppression of Brønsted acidity.

The experimental data are inconsistent with a commonly accepted interpretation according to which sites of one type operate as acid sites, whereas sites of the other type lead to a hydrogenation–dehydrogenation reaction. In this case, an alkane is dehydrogenated to an alkene at a metal site; then, the resulting alkene is isomerized to a branched alkene at an acid site. In turn, the branched alkene is hydrogenated to a branched alkane at the metal site. Because the introduction of platinum results in the disappearance of acidity, the classical mechanism of bifunctional catalysis cannot be used to describe the conversion of alkanes on Pt-containing zeolite catalysts.

Table 3. Spin multiplicity (M), adsorption energy (E_{ads}), charge (q), Fermi level (E_f), band gap (E_{bg}), ionization energy (IE), electron affinity (EA), chemical potential (μ), and hardness (η) for the isolated Pt_6 cluster and the Pt_6 particle in HZSM-5 and EFAL–ZSM-5 zeolites

Cluster	M	E_{ads}, kcal/mol	$q(Pt_6)$	E_f, eV	E_{bg}, eV	IE*, eV	EA*, eV	μ, eV	η, eV
Pt6	9	–	0.0	–5.47	1.43	6.94	2.51	–4.73	2.22
Pt_6/HZSM-5	3	44.7	0.53	–4.43	1.50	5.59	1.82	–3.71	1.89
Pt_6/EFAL	3	58.4	0.31	–5.78	1.31	7.24	3.04	–5.14	2.10
Pt_6/EFAL–ZSM-5	3	49.2	0.08	–4.50	1.41	5.53	1.96	–3.74	1.78

* The ionization energy (electron affinity) was calculated as the energy difference between positively (negatively) charged and neutral clusters. Clusters with a spin multiplicity that corresponded to the lowest energy were used in the calculations.

To explain the high isomerizing activity of Pt/HZSM(15) and Pt/HZSM(38) catalysts, we can invoke a mechanism of hexane conversion on metal-containing catalysts without the direct participation of acid sites [20]. According to this mechanism (see the scheme), surface metal–hexyl structure **2** is formed at the first step of the oxidative addition of *n*-hexane. Alkane addition can occur not only at the first carbon atom, as shown in the scheme, but also at any chain atom to affect the composition of isomerization and cracking products. At the second step, the C–H bond in the hexyl fragment is broken to form propyl–metal–cyclobutane complex **3**. The cleavage of a C–C bond in structure **3** leads to the formation of a complex of a surface carbene and adsorbed pentene (structure **4**). The subsequent transformation of complex **4** can occur either with the formation of isohexane or by cracking.

The isomerization reaction involves the rotation and recombination of adsorbed pentene with the surface carbene to form isopropyl–metal–cyclobutane complex **6**. At the final two steps, the hydrogenation of structure **6** leads to isohexane (in particular, to 2-methylpentane) and active site regeneration. Cracking implies that, after C–C bond cleavage (step **3** ⟶ **4**), the migration of adsorbed pentene in structure **4** occurs with the subsequent hydrogenation of hydrocarbon fragments to form methane and pentane.

Let us consider a simplified energy profile in the triplet state (Fig. 2), which illustrates the key steps of the mechanism of alkane isomerization and cracking in the Pt_6/HZSM-5 system. It includes C–C bond cleavage in metal–cyclobutane complex **I** with the formation of a surface carbene and an adsorbed alkene (structure **II**). The height of the activation barrier at the step of C–C bond cleavage (E_{a1}) is responsible for the activity of the catalyst in alkane conversion. The calculated value of E_{a1} is no higher than 10 kcal/mol, which suggests the high activity of this catalyst, and is consistent with the found high conversions of *n*-hexane. The next steps responsible for the selectivity of alkane conversion are the recombination of the surface carbene and π-coordinated alkene (step **II** ⟶ **I**; the activation energy E_{a2}) and the desorption of the alkene (the desorption energy E_d). The contributions of isomerization and cracking

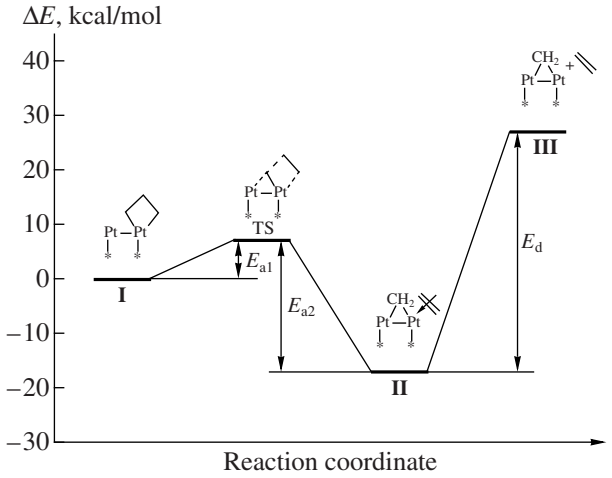

Fig. 2. Energy profile that illustrates the key steps of alkane conversion on Pt_6/HZSM-5 catalysts.

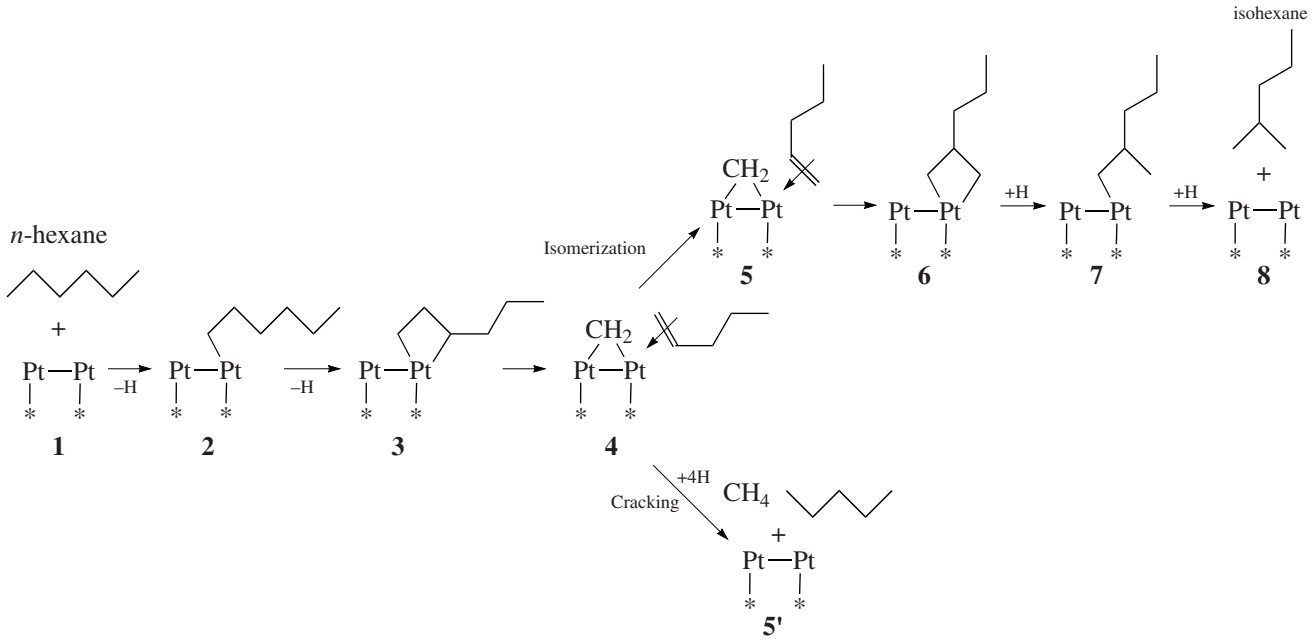

Scheme. Hexane reaction paths on platinum–zeolite catalysts.

reactions depend on the E_d/E_{a2} ratio. The higher this ratio, the greater the contribution of isomerization. The energy diagram indicates that the value of E_d/E_{a2} for the Pt_6/HZSM-5 system is 1.8, which can explain the high selectivity of Pt/HZSM(15) and Pt/HZSM(38) catalysts with respect to the formation of isohexanes (Table 2). The aluminum depletion of the framework is accompanied by a decrease in *n*-hexane conversion and a dramatic decrease in the yield of cracking products. In accordance with the experimental data, we assume that the decrease in the activity is due to a decrease in the acidity of BASs and, consequently, a decrease in the concentration of active structures, which are stabilized $[Pt_nH_m]^{m+}$ complex cations. The almost complete disappearance of C_1–C_5 hydrocarbons from the products of *n*-hexane conversion on the sample with the ratio Si/Al = 38 can be explained by the absence of accessible BASs, which do not interact with platinum, from the catalyst. It is likely that the Pt/HZSM(15) catalyst contains a sufficient amount of BASs that do not interact with the metal, and these BASs are active in cracking.

Data in Table 1 allowed us to find a number of essential differences between the distributions of aluminum in mordenites and ZSM-5 zeolites. In mordenites prepared from alkaline gels by a hydrothermal synthesis, the Si/Al ratio can be varied over a comparatively narrow range (from 5 to 10). The removal of aluminum from the mordenite frameworks by dealumination causes much more radical changes in the composition. The treatment of the NH_4 forms of mordenites preheated at $T \geq 650$°C with acid solutions is the only reliable procedure for the preparation of samples containing a small amount of aluminum (Si/Al > 25). In the course of thermal treatment, a portion of aluminum passes into the extraframework state and then remains in the samples after the subsequent acid treatment. As can be seen in Table 1, more than 50% aluminum atoms transferred to an extraframework state upon the thermal treatment of the ammonium form of zeolite $NH_4M(6)$. The subsequent acid treatment incompletely extracted EFAL; therefore, all of the samples with high degrees of dealumination contained both framework aluminum and EFAL atoms.

The structure of EFAL compounds remains unknown. It is believed that these are hydrated Al^{3+} cations or various oxo compounds containing coordinatively unsaturated aluminum atoms [21]. These aluminum atoms can play the role of LASs. As demonstrated above, the formation of active sites for alkane cracking and isomerization can be related to the interaction between the platinum particle and BAS. Thus, it is very likely that sites active in isomerization are formed as a result of the interaction of the metal with LASs. Figure 1b shows the adsorption complex between the Pt_6 cluster and the extraframework species $Al_2O_2(OH)_2$; in Fig. 1c, this complex is placed in a zeolite channel.

It can be seen that the configuration of a platinum particle was distorted upon adsorption at EFAL: the distance between Pt atoms coordinated to oxygen atoms increased to 3.64 Å; simultaneously, the platinum particle acquired a positive charge because of electron-density transfer to aluminum atoms through oxygen atoms. Comparing the structures of Pt_6/HZSM-5 and Pt_6/EFAL, we can note that the platinum particle adsorbed at EFAL acquired a much smaller charge. The metal particle became strongly polarized: platinum atoms from the lower layer were positively charged (0.27); the charge decreased to 0.09 on atoms from the medium layer, whereas atoms in the upper layer bore a negative charge (–0.20). As in the case of BASs, the spin multiplicity of the platinum particle decreased to 3 upon adsorption at EFAL; in this case, the stabilization energy of the metal cluster was higher than 58 kcal/mol. The interaction of platinum with EFAL resulted in an increase in the chemical potential by 0.41 eV and a small decrease in the hardness. Upon the introduction of the Pt_6/EFAL complex into the zeolite channel, the adsorption energy of the particle decreased to 49 kcal/mol; moreover, the total charge of the platinum particle decreased to 0.08 because of an electron-density redistribution from framework silicon atoms through basic oxygens.

The Pt_6 cluster in the structure of Pt_6/EFAL–ZSM-5 was much less polarized than that in the Pt_6/EFAL complex. The chemical potential and hardness of the cluster arranged in a channel decreased by 1.4 and 0.32 eV, respectively. The Pt_6/EFAL–ZSM-5 complex was characterized by the triplet ground state, and the singlet–triplet splitting was no higher than 3 kcal/mol. Thus, except for charge, platinum particles that interact with BASs and EFAL exhibited very similar electronic structures. Therefore, we believe that these particles will exhibit similar activities in C–C bond cleavage.

Let us see how the formation of various EFAL amounts affects the catalytic properties of dealuminated mordenites in *n*-hexane conversion. In Table 2, it can be seen that, as aluminum was removed from the zeolite framework, the activity of mordenites initially increased to reach a maximum and then decreased. Usually, this character of changes in the course of dealumination is due to the increase in the strength of BASs, which reaches a maximum after the removal of about half of the atoms from the framework (Fig. 3a). However, this explanation is based on the hypothesis that aluminum occurs entirely in the framework, and it ignores the formation of extraframework compounds and the interactions of the metal with BASs and LASs. Nonetheless, the separate determination of framework aluminum and EFAL showed that the sample containing only 1.3 framework aluminum atoms and 3 EFAL

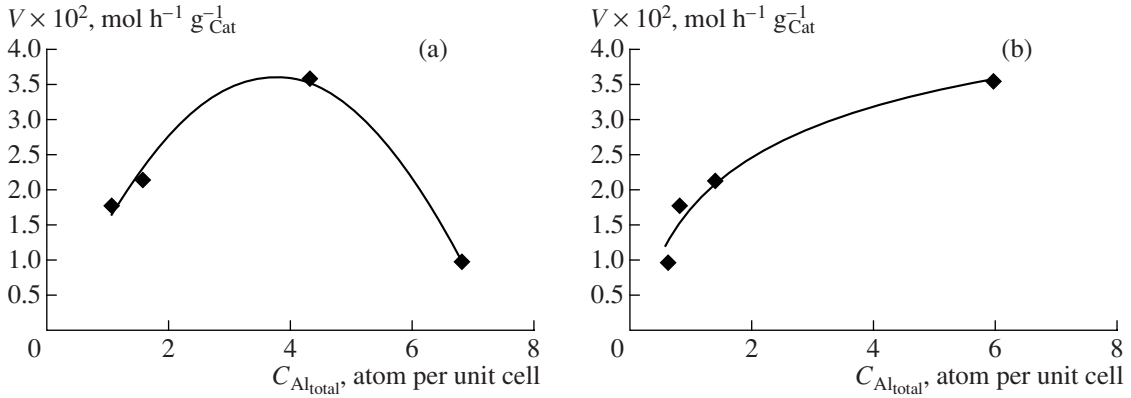

Fig. 3. Dependence of the rate of *n*-hexane isomerization on the aluminum content of the sample: (a) total aluminum (Al_{total}) and (b) EFAL in mordenite (Al_{extra}).

atoms per unit cell exhibited a maximum activity in isomerization. The plot in Fig. 3b reflects the well-defined correlation between the activity and the number of EFAL atoms in the unit cell.

It is most likely that the reactions of hydrocarbon conversion on mordenites occur near the outer surface. Therefore, the major portion of acid sites is arranged far from platinum particles, and, for this reason, it does not participate in the formation of active sites. Upon dealumination, on the one hand, an additional system of micro- and mesopores is formed, and, on the other hand, additional LASs are formed. Correspondingly, new active sites are formed by the interaction of platinum particles with the resulting EFAL compounds and previously inaccessible BASs; this leads to an increase in activity upon the removal of half of the aluminum from the framework. Upon deeper dealumination, the total number of acid sites (BASs and LASs) decreases dramatically and a decrease in the catalytic activity is observed. The high catalytic activity of the DHM(9.5) catalyst, which contains only 1.3 framework aluminum atoms per unit cell, suggests the important role of LASs in the formation of active sites for *n*-hexane conversion in dealuminated mordenites. Thus, a decrease in the number of BASs in dealuminated samples is compensated by the formation of LASs, which interact with platinum as readily as proton sites do. According to data in Table 3, the platinum particle adsorbed at an LAS bears a somewhat smaller charge than the cluster adsorbed at a BAS does. On the assumption that the relative stability of complex **4** (scheme) is the same for both Pt/BAS and Pt/LAS, the selectivity of *n*-hexane conversion is primarily related to the olefin desorption energy (E_d). Because an increase in the particle charge leads to an increase in E_d, the Pt/LAS centers would be expected to make a somewhat greater contribution to cracking.

Thus, the integrated study of *n*-hexane conversion on Pt-containing dealuminated mordenites and ZSM-5 zeolites demonstrated that the introduction of platinum into high-silica zeolites results in the formation of active sites as oxidized platinum particles stabilized at BASs or LASs. The interaction of a platinum cluster with acid sites leads to the suppression of the acidity of the support. The mechanism of alkane conversion on sites of this type implies the formation of metal–cyclobutane and metal–carbene intermediates, and it does not require the direct participation of acid sites. The data obtained can be used in the analysis of hydrocarbon conversions on other metal-containing catalysts.

REFERENCES

1. Blomsa, E., Martens, J.A., and Jacobs, P.A., *Stud. Surf. Sci. Catal.*, 1997, vol. 105, p. 909.
2. Mishin, I.V., Reschetilovski, W., Rubinstein, A.M., and Vendlandt, K.P., *Z. Anorg. Allg. Chem.*, 1980, vol. 467, p. 381.
3. *Catalysis and Zeolites: Fundamentals and Applications*, Weitkamp, J. and Puppe, L., Eds., Berlin: Springer, 1999.
4. Mishin, I.V., Kapustin, G.I., and Brueva, T.R., *Kinet. Katal.*, 1997, vol. 38, no. 4, p. 626 [*Kinet. Catal.* (Engl. Transl.), vol. 38, no. 4, p. 574].
5. Weisz, P.B. and Swegler, E.W., *Science*, 1957, vol. 126, p. 31.
6. Kuhlmann, A., Roessner, F., Schwieger, W., Gravenhorst, O., and Selvam, T., *Catal. Today*, 2004, vol. 97, p. 303.
7. Ono, Y., *Catal. Today*, 2003, vol. 81, p. 3.
8. Mikhailov, M.N., Kustov, L.M., and Mordkovich, V.Z., *Izv. Akad. Nauk, Ser. Khim.*, 2007, no. 3, p. 386.
9. Kubicka, D., Kumar, N., Venäläinen, T., et al., *J. Phys. Chem. B*, 2006, vol. 110, p. 4937.
10. Mishin, I.V., Baier G-K., Karge G.G., *Kinet. Katal.*, 1993, vol. 34, p. 156.
11. Becke, A.D., *J. Chem. Phys.*, 1993, vol. 98, p. 5648.
12. Lee, C., Yang, W., and Parr, R.G., *Phys. Rev. B: Condens. Matter*, 1988, vol. 37, p. 785.

13. Vosko, S.H., Wilk, L., and Nusair, M., *Can. J. Phys.*, 1980, vol. 58, p. 1200.
14. Stevens, W.J., Krauss, M., Basch, H., and Jasien, P.G., *Can. J. Chem.*, 1992, vol. 70, p. 612.
15. Schmidt, M.W., Baldridge, K.K., Boatz, J.A., Elbert, S.T., Gordon, M.S., Jensen, J.J., Koseki, S., Matsunaga, N., Nguyen, K.A., Su, S., Windus, T.L., Dupuis, M., and Montgomery, J.A., *J. Comput. Chem.*, 1993, vol. 14, p. 1347.
16. Granovsky, A.A., *PC GAMESS, Version 7.1*, http://classic.chem.msu.su/gran/gamess/index.html.
17. Glendening, E.D., Badenhoop, J.K., Reed, A.E., Carpenter, J.E., and Weinhold, F., *NBO 4.M*, Madison: Theoretical Chemistry Institute, University of Wisconsin, 1999.
18. Olson, D.H., Lago, R.M., and Haag, W.O., *J. Catal.*, 1980, vol. 61, p. 390.
19. Parr, R.G. and Pearson, R.G., *J. Am. Chem. Soc.*, 1983, vol. 105, p. 7512.
20. Mikhailov, M.N., Kustov, L.M., and Kazansky, V.B., *Catal. Lett.*, 2008, vol. 120, p. 8.
21. Benco, L., Bucko, T., Hafner, J., and Toulhoat, H., *J. Phys. Chem. B*, 2005, vol. 109, p. 22 491.